

**PDR TRIP REPORT**

LPDR

Distribution:

TO: King Stablein, PM NNWSI		TRAVELER	
Through: (Return to WM, 623-SS) Paul Prestholt, OR, NNWSI		Charlotte Abrams, Keith McConnell, and	
PLACES VISITED		BRANCH	
US Geological Survey Offices, Denver, CO		Bakr Ibrahim, WMGT	
PERSONS CONTACTED		DATES OF TRIP	
USGS Personnel: Bob Raup, William Dudley, Robert Scott, John Stuckless, Mariett Rehels, Florian Maldonado, Brad Meyers, John Whitney, Steve Harmsen, Ken Fox, Sam Harding, and Hans Ackerman		8/25/86 to 8/28/86	
PURPOSE OF TRIP			
To talk with members of the USGS staff assigned to the NNWSI project and to get an overview of the status of previous, current and ongoing work in the areas of geology and geophysics.			
ACCOMPLISHMENTS			
USGS staff orally presented details of their work on the NNWSI project and allowed NRC staff to view maps and logs in progress. NRC staff's questions on the status of current work on vein deposits, structure, tectonics, and geophysics were answered and NRC staff members received a clear picture of current geologic work at the Yucca Mountain Site.			
PROBLEMS ENCOUNTERED			
None, the USGS staff were very helpful in answering the NRC staff's questions and in making NNWSI assigned staff available for interaction.			
PENDING ACTIONS			
The NRC staff will make use of the knowledge gained in this interaction in preparations for a planned NRC/DOE seismo-tectonics meeting.			
RECOMMENDATIONS			
Due to the lag time between completion of work and publication by the USGS these type interactions are necessary for NRC staff to remain cognizant of ongoing NNWSI work. Continuation of these type interactions may facilitate a timely exchange of ideas and concerns between the NRC and DOE.			
SIGNATOR (TRAVELER)		DATE	
Charlotte Abrams		9/4/86	

B612010433 860904  
PDR WASTE  
WM-11 PDR

87030077F M

DATE 9/4/86

concurrency by P. Prestholt, OR 9/9/86 by phone

1190

To be published by  
Seismological Society of  
America

**Inferences about the local stress field from focal mechanisms:  
applications to earthquakes in the southern Great Basin of Nevada**

by S. C. Harmsen and A. M. Rogers

**Abstract**

Focal mechanisms determined from regional-network earthquake data or aftershock field investigations often contain members ranging from strike slip to normal slip in extensional tectonic environments or from strike slip to thrust slip in compressional environments. Although the coexistence of normal and strike-slip faulting has suggested to some investigators that the maximum and intermediate principal stresses are of approximately equal magnitude, several have asserted that the directions of principal stresses can or must interchange to accommodate both types of mechanisms (Zoback and Zoback, 1980b; Vetter and Ryall, 1983). A Coulomb-Navier criterion of slip is invoked to demonstrate that both types of mechanisms, as well as oblique members having preferred nodal-plane dips intermediate between those of the strike-slip and normal mechanisms, may be observed in a region where the stress field, resolved into principal components, is axially symmetric. The proximate coexistence of earthquakes having diverse focal mechanisms could be interpreted as evidence for an approximately axially symmetric stress field in a region where optimally oriented planes of weakness are known to exist in the host rock.

**Introduction**

The regional stress field in the region surrounding Yucca Mountain, Nevada Test Site, must be determined to assess the suitability of that site for a potential nuclear waste repository. Small earthquakes in the southern Great Basin of Nevada and California sometimes provide enough first-motion P-wave polarity information and SV/P amplitude information to closely constrain the quadrantal pattern or nodal planes of focal mechanisms. In this study we wish to examine how these mechanisms can be used to infer properties of the regional acting stress field. Figure 1 presents a set of strike-slip, oblique-slip, and normal mechanisms that were obtained using data collected from the southern Great Basin regional seismograph network (Rogers *et al*, 1983; A. M. Rogers, written comm., 1985). The average station spacing is about 20-30 km; most earthquakes

for which mechanisms are computed have estimated depth-of-focus error less than 2 km. There is little if any correlation of mechanism type with estimated depth-of-focus, ranging from near-surface to about 10-15 km. The question of immediate practical interest is, "Does the occurrence of this suite of mechanism types over the aperture of the network and throughout the seismogenic crust contain unequivocal information about the magnitudes or orientations of the acting principal stresses?" Experimental laws and results drawn from the field of rock mechanics will be used to provide a model for associating focal mechanisms with stress fields, and using this model, we will make some observations about stress regimes that are likely to be present given certain fault types or sets of focal mechanisms.

Figure 1 near here

The determination of an average stress field acting in a given region from inversion of paleostrain or focal mechanism data has been receiving increasing attention (e.g., Angelier, 1979; Gephart and Forsyth, 1984; Michael, 1984). Most paleostrain investigations have concentrated on rotating plausible initial stress fields until a measure of misfit such as  $\sum_{k=1}^N \sin^2(\frac{\alpha_k}{2})$  or  $\sum_{k=1}^N \min[\tan^2(\alpha_k), 1]$  is minimized, where  $\alpha_k$  is the angle between the direction of resolved shear stress on the  $k$ th fault plane and the direction of measured slip on that fault plane, and  $N$  is the number of faults in the sample (Angelier, 1984). Focal mechanism investigations proceed similarly, except that two nodal planes must be considered for each mechanism, and the preferred plane relative to the stress field is identified because the angles  $\alpha_k$  on the two nodal planes are usually different. The preferred plane is the one for which the slip direction most nearly coincides with the resolved shear stress direction. When a stress field (possibly not unique), specified by three principal stress directions and the ratio  $R \equiv \frac{\sigma_1 - \sigma_2}{\sigma_1 - \sigma_3}$ , has been found that minimizes the misfit between slip directions and resolved shear stress directions for the largest possible subset of slip data, that stress field is presumed to be an acceptable approximation to the actual local stress field. We here designate the condition of the vanishing of tangential stress on the fault plane in the direction perpendicular to the direction of slip as criterion I.

Many parameter studies (e.g., Sibson, 1974; Zoback and Zoback, 1980a) and inversions (Michael, 1984) have applied frictional sliding criteria rather than criterion I above to relate paleoslip or focal mechanism data to the acting stress field. This procedure is justified because slip on preexisting

fractures and faults occurs before brittle fracture of the rock mass as a whole; furthermore, such slip appears to conform to a simple law (Byerlee's law) over a wide variety of rock types, temperatures, surface roughnesses, confining pressures and pore pressures.

In this paper, a second constraint brought to bear in the search for the "best-fitting" stress field is inferred from the Coulomb-Mohr-Navier law of frictional sliding in faulted rock. The Coulomb-Mohr criterion of frictional sliding on preexisting planes of weakness states that

$$|\tau_{xy}| = S_0 + \mu\sigma_{eff} = S_0 + \mu(\sigma_n - P), \quad (1)$$

where  $\tau_{xy}$  is the tangential traction needed to overcome static friction,  $S_0$  is the cohesion, and  $\mu$  is the coefficient of friction; and the effective normal stress  $\sigma_{eff}$  is the normal stress across the fault plane  $\sigma_n$ , reduced by pore pressure  $P$ .  $x$  is the slip direction and  $y$  is the direction normal to the fault plane. Criterion II, as applied in this discussion, is that slip on a preexisting fault will occur only if the fault is oriented such that the ratio of  $\tau_{xy}$  to  $\sigma_{eff}$  attains its maximum possible value for a given stress field (Coulomb-Navier hypothesis). In the analysis that follows, a focal-mechanism nodal plane is assumed to be a permissible fault plane for a given stress field only if criterion II holds on that nodal plane. For a given sample of focal mechanisms, criterion II determines the best-oriented fault planes for frictional sliding, and criterion I determines the direction of sliding on those planes. A third criterion tacitly satisfied in the discussion which follows is that the resolved shear stress on each permissible fault plane must agree with the sense of slip on the fault.

The following general questions will be addressed here: what is the maximum variation in style and orientation that may be expected in focal mechanisms or other slip data meeting criteria I and II, and under what stress field conditions should this maximum variation be observed? The maximum variation will be shown to occur in axially symmetric stress fields; i.e., fields in which two of the three principal stresses have equal magnitudes. The association of observed focal mechanisms at Black Mountain (Figure 1) with one such axially symmetric stress field will be postulated, using the assumption that criteria I and II are valid in that region.

To avoid the introduction of complications, the rock volume in which earthquakes are occurring is assumed to be homogeneous and isotropic, except for the presence of faults. This simplification allows us, using the minimum number of independent parameters, to map the observed strain field members (i.e., P and T axes of focal mechanisms) into the stress field. A recent discussion

of the mapping will be found in Gephart (1985). The stress field is described by three principal stress directions,  $\hat{\sigma}_1, \hat{\sigma}_2$ , and  $\hat{\sigma}_3$ , whose magnitudes are  $\sigma_1, \sigma_2$ , and  $\sigma_3$ , respectively. Although in the earth's crust the stress field is known to change with position, due to geographically changing gravitational and tectonic components, rock anisotropies, and due to the presence of interacting faults, in this study a regional stress field is assumed to exist that can be represented by fixed mean principal stress directions. No information concerning principal stress magnitudes is contained in earthquake focal mechanisms. Fortunately, stress magnitudes are not needed for this analysis; however, the ratio of minimum effective compressive stress,  $\sigma_3 - P$ , to maximum effective compressive stress,  $\sigma_1 - P$ , is required and is fixed at a value in conformity with laboratory data on friction in rocks (e.g., Byerlee, 1978). Generally, for any orientations of principal stresses, this ratio is closely related to the rock-failure or fault-stability parameters (e.g., Jaeger and Cook, 1969; Sibson, 1974; Zoback and Healy, 1984):

$$\frac{\sigma_3 - P}{\sigma_1 - P} = \frac{1}{[(\mu^2 + 1)^{1/2} + \mu]^2} \quad (2)$$

This equation follows from the assumptions that  $\mu = \max_{\Phi} \frac{|\tau_{xy}|}{\sigma_{eff}}$  and that  $S_0 \ll \mu \sigma_{eff}$ , where  $\Phi$  is the acting stress tensor, and  $\sigma_{eff}$  is the normal stress on the fault, reduced by the local pore pressure. Equation (2) will be assumed to be valid. If planes of weakness having optimal orientation for sliding are available in the region, slip should locally decrease deviatoric stresses so that  $\tau/\sigma_{eff}$  should never exceed  $\mu$  on any planes. Therefore, the assumption that  $\mu$  is equal to  $\max \frac{|\tau_{xy}|}{\sigma_{eff}}$  may be a physically plausible relationship between active faults and the stress field which activates them, at least in highly faulted seismogenic regions, at depths where  $S_0$  may be considered negligible when compared to  $\sigma_{eff}$ , i.e., depths greater than 3 km.

For most of the following discussion, we restrict consideration to stress fields in which  $\sigma_2$  is in the direction of B. (Although this restriction appears to be arbitrary, it is implied by criterion II, i.e., planes on which  $\max_{\Phi} |\tau_{xy}|/\sigma_n$  is achieved are parallel to the intermediate principal stress axis.) Stresses may be considered effective stresses or dry-rock stresses. Gephart (1985) showed that for all focal mechanisms having null (B) axes parallel to the intermediate principal stress direction,  $\hat{\sigma}_2$ , and pressure (P) and tension (T) axes in the same dihedral as  $\sigma_1$  and  $\sigma_3$ , respectively, criterion I is automatically satisfied for both nodal-plane slip vectors for all magnitudes of  $\sigma_1, \sigma_2$ , and  $\sigma_3$ ; i.e., for all values of  $R$ ,  $0 \leq R \leq 1$ . In the analysis below, two assertions will be demonstrated by

example. First, for each of those mechanisms, criterion II either restricts the directions,  $\hat{\sigma}_1$  and  $\hat{\sigma}_3$ , to essentially unique locations on the focal hemisphere or excludes the mechanism altogether. Second, for certain sets of focal mechanisms associated with the same stress field, criterion II completely removes the ambiguity in fault-plane identification when  $\mu > 0.6$ . Zoback and Healy (1984) argued against  $\mu < 0.6$  for faulted rock at mid-crustal depths.

#### Focal Mechanisms and Associated Stress Fields: Examples

Certain focal mechanisms are considered on the basis of their similarity to many of the focal mechanisms determined from southern Great Basin earthquakes. A range of principal stress directions that might be acting is applied and constrained so that  $\sigma_1$  lies in a dilatational quadrant and  $\sigma_3$  lies in a compressional quadrant (McKenzie, 1969). This range includes the inferred principal stress directions of previous investigations in the Nevada Test Site region (Stock *et al*, 1985, Table 3). In particular, a variety of measurements indicates northwest to west-northwest extension, in agreement with the mean direction of the T axes of the 29 focal mechanisms shown in Figure 1. Figure 2 shows the distribution of P and T axes for those mechanisms, and their distribution indicates that the mean regional direction of maximum shortening is less well-constrained than the direction of maximum elongation. We will present a stress field consistent with those mean strain directions.

Figure 2 near here

We first examine the range of principal stress directions that may be associated with a given focal mechanism when  $\mu$  is known and  $S_0 \approx 0$ , initially considering the set of stress fields such that  $\sigma_2$  is oriented vertically, and subsequently considering fields such that  $\sigma_1$  is oriented vertically. The stress field is further constrained by fixing the magnitude of  $\sigma_3 = k\sigma_1$ ,  $0.24 \leq k \leq \frac{\nu}{(1-\nu)} = 0.316$ , where  $\nu = \text{Poisson's constant} = 0.24$ , corresponding to  $V_P/V_S = 1.71$ , obtained for several southern Great Basin earthquakes using the Wadati method (Rogers *et al*, 1983). The upper bound on  $k$  represents a commonly assumed relationship between maximum and minimum principal stresses that is obtained from the linear elastic equations, assuming that gravity is the source of the stress field. This value results when (1)  $\sigma_1$  is oriented vertically and has magnitude equal to that of the overburden, (2) the rock volume is constrained to have zero lateral displacement at its boundaries, and (3) pore pressure is zero (Jaeger and Cook, 1969). The lower bound on  $k$  might apply when a small tectonic component of extension is diminishing the minimum horizontal stress from the

purely gravitational level, once again assuming that  $\sigma_1$  is vertically oriented. Alternatively, the same bounds on  $k$  might exist for the model  $(\sigma_3 - P) = k(\sigma_1 - P)$ , where now  $P > 0$  but the magnitude of  $\sigma_3$  is closer to that of  $\sigma_1$ . Although no tectonic-gravitational explanation is provided for this latter model, available evidence summarized by Stock *et al* (1985, Table 1) shows that  $P$  is often about half the minimum horizontal stress at shallow depths at Yucca Mountain; furthermore, the minimum horizontal stress is about half the vertical stress, so that if these represent principal stresses,  $k \approx 0.33$ . If topographic boundary conditions are rotating the principal stress directions away from vertical and horizontal (Savage *et al*, 1985), then  $k < 0.33$ .

The first focal mechanism analyzed has a north-striking, vertically dipping fault plane with right-lateral slip and an east-striking, vertically dipping plane with left-lateral slip. Figure 3a shows the mechanism and the stress directions considered. Criterion I is satisfied on both nodal planes, regardless of the direction of  $\sigma_1$  or the magnitude of  $\sigma_2$  (as long as  $\sigma_1$  remains in the pressure quadrants). Figure 3b shows that, for the range of generally acceptable  $\mu$  values, that is,  $0.6 < \mu < 0.9$  (Morrow and Byerlee, 1984), slip is possible on the north-south plane for  $\sigma_1$  orientations greater than about  $13^\circ$  and less than  $45^\circ$  when  $k \leq 0.24$ . When  $k \geq 0.32$  a much narrower range of  $\sigma_1$  orientations would be favorable. (Note that if pore pressure is increased, the effect is to raise the level of these curves and expand the range of  $\sigma_1$  orientations under which slip is possible on both the north-south and east-west planes; also  $\max \frac{\tau}{\sigma_n}$  is shifted.) If we assume that faults of optimal orientation are available to relieve stress, then  $\frac{\tau}{\sigma}$  could never exceed  $\mu$  and sliding would only occur for  $\sigma_1$  oriented such that  $\frac{\tau}{\sigma}$  is maximized. This assumption is criterion II.

Figure 3 a,b near here

Using this assumption, for the case  $k = 0.24$ , the maximum value of  $\tau_{xy}/\sigma_{eff}$  is 0.776, and slip on the north-south plane only occurs when the direction of  $\sigma_1$  is  $N26^\circ E$ . For the case  $k = 0.316$ , a maximum of  $\tau_{xy}/\sigma_{eff}$  of 0.608 occurs at  $\theta = 29^\circ$ ; i.e., when  $\sigma_1$  is oriented at  $N29^\circ E$ . Thus our upper bound on  $k$  represents the lower bound for generally accepted  $\mu$  values. Note that  $\tau/\sigma$  on the east-west plane is much lower (due to a larger normal stress across that plane) than on the north-south plane, thus eliminating most ambiguity in the identification of the preferred plane when principal stress directions are approximately known. These sets of principal stress directions are in agreement with the suggestion of Raleigh *et al* (1972), that given a preferred nodal plane,

the most-likely direction of maximum principal stress falls in the region about  $60^\circ$  to the nodal plane normal and  $30^\circ$  to the slip direction.

A commonly held view in earthquake seismology is that the focal mechanism P axis, or its horizontal projection, is a reasonable estimate for the direction of  $\sigma_1$ . Note from Figure 3b that  $\tau/\sigma \leq 80\%$  of its maximum value when  $k \leq 0.24$  and  $\sigma_1$  is parallel to P ( $\theta = 45^\circ$ ), perhaps indicating that such an arbitrary choice of principal stress directions is not always justifiable. In defense of such a position, however,  $\tau_{xy}$  is maximized when  $\sigma_1$  is parallel to P and  $\sigma_{eff}$  is equal on the two nodal planes, so that if little is known about principal stress directions, no fault plane preference is introduced by setting  $\sigma_1$  parallel to P. Also, failure of some sedimentary rock is known to approximately obey Tresca's criterion (Jaeger and Cook, 1969) which states that principal stress axes coincide with the axes of maximum strain. The seismological implications of the theory that fracture occurs on planes of maximum shearing stress are discussed by Ben-Menahem and Singh (1981, pp 190-194).

Having established a unique set of principal stress directions for which criteria I and II are satisfied for horizontal slip on the north-south nodal plane of Figure 3a (*unique* in a mathematical sense; given the uncertainties in data and physical properties, all solutions are approximate), we next characterize the other members of the set of fault planes and slip directions that also may be associated with those stress directions. For the stress field in which  $k = 0.24$  and  $\theta = 26^\circ$ , the conjugate fault to the north-south plane exhibiting right lateral strike slip is the north- $52^\circ$ -east plane exhibiting left lateral strike slip. These strike-slip solutions satisfy criteria I and II no matter what the relative magnitude of  $\sigma_2$  is. Thus criteria I and II provide a model for conjugate fault systems that are frequently observed in geological field studies. An unfortunate ambiguity of usage of the word "conjugate" is that in seismology, the focal-mechanism nodal planes are said to be conjugate (e.g., Ben-Menahem and Singh, 1981, p 182), but in geology, pairs of fault planes both satisfying criterion II or some allied law such as equation (3) below are said to be conjugate. This discussion adopts the geological connotation, with the implication that the angle between conjugate fault planes is acute ( $\approx 50^\circ$  to  $70^\circ$ ).

For the same orientations of principal stress axes, we now restrict  $\sigma_2$  to various specific amplitudes. When  $\sigma_2 = \sigma_1$ , faults exhibiting normal and oblique slip also satisfy criteria I and II relative



to that stress field and might be considered equally as likely to rupture as the strike-slip faults. Figure 4 shows the range of focal mechanisms and preferred nodal planes that can be associated with such an axially symmetric stress field when  $\sigma_2 = \sigma_1$ .

Figure 4 near here

The pure dip-slip mechanisms may appear peculiar in that their B axes are parallel to  $\hat{\sigma}_1$ ; but for these cases,  $\sigma_2$ , which is vertically oriented, takes the role of  $\sigma_1$ . The set of focal mechanisms is described by the facts that their B axes are in the stress-field plane of symmetry and that the slip vectors of the preferred nodal planes subtend an angle of  $26^\circ$  with that plane of symmetry. There is no component of thrust on any slip vector in the set. The principal conclusion is that given these principal stress directions and relative magnitudes, slip on optimally oriented pre-existing faults will range from strike slip on vertically dipping faults, to oblique normal slip on faults dipping  $70^\circ - 85^\circ$ , to pure normal slip on faults dipping  $60^\circ - 65^\circ$ .

Essentially three other axially symmetric stress fields have vertical and horizontal principal stress directions. The field in which  $\sigma_1$  is vertical and  $\sigma_2 = \sigma_3$  admits only dip-slip mechanisms of arbitrary strike using the criteria assumed. The dip of the preferred planes is fixed by the value of  $k$  or, more generally, by  $\frac{\sigma_2 - P}{\sigma_1 - P}$ . The field in which  $\sigma_3$  is vertical and  $\sigma_1 = \sigma_2$  admits only pure reverse-slip mechanisms. Finally, the field in which  $\sigma_2$  is vertical and  $\sigma_3 = \sigma_1$  admits a set of mechanisms similar to those of Figure 4, where now the range of rock deformation is strike slip to reverse slip, shown in Figure 5.

Figure 5 near here

That the maximum range of faulting styles will be observed only in axially symmetric stress fields follows from equation (2), which implies that the angle  $\phi$  between the normal to a favorably oriented fault plane and  $\hat{\sigma}_1$  is

$$\phi = 0.5 \left[ \frac{\pi}{2} + \tan^{-1} \mu \right], \quad (3)$$

and the intermediate stress,  $\sigma_2$ , is in the plane of the fault (Jaeger and Cook, 1969). When  $\sigma_1 = \sigma_2$ ,  $\phi$  is determined not just from  $\sigma_1$ , but from any axis in the plane of  $\sigma_1$  and  $\sigma_2$ . For each fault plane, criterion I admits only one slip direction. Thus, rigorous application of both criteria in a given triaxial stress field in which no two principal stress magnitudes are equal would admit only two conjugate fault planes and slips, as discussed by Anderson (1951).

Although only two faults, each having a fixed slip direction, satisfy criteria I and II in a stress field in which  $R \neq 0$  and  $R \neq 1$ , stress fields can sometimes be found that approximately satisfy criteria I and II for data sets having some variation in fault trend and dip. Relaxation of criterion II by admitting faults having  $\frac{\tau}{\sigma_n} < \max \frac{\tau}{\sigma_n}$  results in the association of a larger collection of favorably oriented faults with a given triaxial stress field. Paleostress and focal-mechanism inversions often ignore criterion II altogether, but by concentrating on finding stress fields that approximately fit criterion I, they may produce solutions for which many of the slip data are in serious disagreement with equations (1) and (2) for any reasonable  $k$ . To illustrate why criterion II needs to be at least approximately satisfied, we consider the strike-slip mechanism and principal stress directions of figure 3a again, except that we now permute the  $\sigma_1$  and  $\sigma_2$  axes, so that  $\sigma_1$  is vertical. Figure 6 shows the relationship between  $\frac{\tau}{\sigma}$  and  $\theta$ , the angle between  $\sigma_2$  and the north-south nodal plane. Criterion I is satisfied on both nodal planes for all values of  $R : 0 \leq R \leq 1$ . (Although  $\sigma_1$  is not now in a pressure quadrant, very small perturbations of stress directions that put  $\sigma_1$  in a pressure quadrant would not substantially alter Figure 6; the smoothness of the direction cosine functions used in determining  $\frac{\tau}{\sigma}$  and the fact that  $\sigma_{eff} > \sigma_3 - P > 0$  guarantee this.) Figure 6 shows that when  $k = 0.24$  and  $\sigma_2$  is oriented at  $26^\circ$  east-northeast,  $\frac{\tau}{\sigma}$  is maximized for  $\sigma_2 = \sigma_1$  (i. e.,  $R = 0$ ), but  $\frac{\tau}{\sigma}$  falls rapidly as  $\sigma_2 \rightarrow \sigma_3$  (i. e.,  $R \rightarrow 1$ ). On vertically dipping north-trending faults having  $\mu > 0.6$ , sliding should not occur unless  $\frac{\sigma_2}{\sigma_1} > 0.75$  (i.e.,  $R < 0.3$ ). In this sense, the condition  $\frac{\tau}{\sigma_n} \approx \max \frac{\tau}{\sigma_n}$  constrains  $R$  almost as much as criterion I does (Gephart, 1985, eq. 3) for any given fault when  $\sigma_2$  is not in the plane of the fault. Using a constraint similar to criterion II to invert several paleoslip samples, Michael (1984) showed that stress direction and  $R$  estimates obtained were similar to those obtained from inversions using criterion I only.

Figure 6 near here

Figure 6 illustrates that strike-slip faulting on steeply dipping planes is not consistent with a stress field having a vertically oriented maximum principal stress, unless the intermediate stress ( $\sigma_H$ ) and vertical stress ( $\sigma_v$ ) have nearly equal magnitudes. The shallow-crust stress field at Yucca Mountain in which  $\sigma_H$  is about halfway between  $\sigma_v$  and  $\sigma_h$  (minimum horizontal stress) (Stock *et al.*, 1985) is probably anomalous when compared to the regional stress field that is producing many strike-slip earthquakes. The directions of  $\sigma_h$  ( $\approx N65^\circ W$ ) and  $\sigma_H$  ( $\approx N25^\circ E$ ) observed at Yucca

Mountain agree well with right-lateral slip on north-trending faults, assuming  $\sigma_H \approx \sigma_v$ ,  $k < 0.25$ , and  $\mu > 0.75$  regionally. Normal faulting at Black Mountain and in the Silent Canyon Caldera (Hamilton and Healy, 1969) are also explained by those stress directions and amplitudes. Ege (1977) reviewed geological evidence suggesting an axially symmetric stress field at Rainier Mesa, in the northern Nevada Test Site. Furthermore, *in situ* stress measurements in welded tuffs at Rainier Mesa, obtained from overcoring, indicate that the maximum horizontal stress equals the vertical stress at very shallow depths (400 m) (Ege, 1977).

The association of a triaxial stress field with both strike-slip and normal focal mechanisms has been shown to satisfy criteria I and II only when the two largest principal stresses are equal, and has been shown to approximately satisfy criterion II when  $\sigma_2 > 0.75\sigma_1$ , in the sense that  $\frac{\tau}{\sigma_n} \geq 0.77 \max \frac{\tau}{\sigma_n}$  on favorably oriented planes. Where such axially symmetric stress fields are present, it is unnecessary to assume that the maximum shear stress required to initiate strike-slip faulting is higher than that required to initiate oblique or normal faulting (contrast with Sibson, 1974, and Smith and Bruhn, 1984).

For observed samples of focal mechanisms or slickensides, such geometric restrictions as the requirement that all fault planes be parallel to  $\hat{\sigma}_2$  must be relaxed if the slip data are to be associated with a fixed stress tensor. The next question that we answer is, "What is the maximum variation in fault-plane orientations for stress fields in which  $\sigma_2$  is midway between  $\sigma_1$  and  $\sigma_3$  ( $R = 0.5$ ), assuming that a fault is favorably oriented when  $\frac{\tau}{\sigma_n} \geq 0.9 \max \frac{\tau}{\sigma_n}$ ?" Computer searches through potential focal mechanisms, at least one of whose nodal plane solutions satisfies criterion I, reveal that the requirement that  $\frac{\tau}{\sigma_n} \geq 0.9 \max \frac{\tau}{\sigma_n}$  still eliminates most of the range in rake of admissible slip vectors on faults in stress fields having  $k \leq 0.25$  and  $R \approx 0.5$ . When  $\sigma_1, \sigma_2$ , and  $\sigma_3$  are oriented as in Figure 3a, the strike-slip mechanisms of Figure 4 are "optimal" ( $\frac{\tau}{\sigma_n} = \max \frac{\tau}{\sigma_n}$ ), but the resolved normal component of slip on all admissible nodal planes is less than 40% of the strike-slip component; i.e., the rake angle  $\leq 22^\circ$  from horizontal on the most shallow-dipping admissible planes, dipping  $73^\circ$ . The preferred nodal planes are still easily identified even when criterion II is relaxed. Because  $\sigma_2$  is generally not parallel to either nodal plane, criterion I is only satisfied on the preferred plane (Gephart, 1985).

#### Axially Symmetric Stress Fields and Tectonic Models

More direct techniques than focal mechanism and paleoslip inversions, such as *in situ* stress measurements, fail to resolve whether axially symmetric stress fields are present, owing to the difficulties in obtaining reliable estimates for  $\sigma_2$  from these measurements (e.g., Stock *et al*, 1985). The triaxial stress field model that permits the interchange of the  $\sigma_1$  and  $\sigma_2$  directions at some depth, due to the gravitational stress gradient with depth being greater than the tectonic stress gradient (Vetter and Ryall, 1983), must accommodate the fact that by continuity, an axially symmetric field must exist at some intermediate depth range; therefore, over this depth range, the variety of mechanisms exhibited in Figure 3 may be observed. As an alternative to two distinct triaxial crustal stress fields separated by an axially symmetric field, the partitioning of mechanism types into strike-slip members at shallow depths and dip-slip members at mid-crustal depths, such as was observed by Vetter and Ryall (1983), can be explained by a preponderance of more steeply dipping planes of weakness near the surface, and more shallow-dipping planes at depth, without invoking permutations of principal stress directions with depth. Such a situation might be expected where listric and detachment faulting are the main sources of the fracture planes. In any case, if criterion II is approximately valid, the separation of events into sets that are either essentially strike-slip or normal, based solely on stress-direction permutation, requires a large change in  $R$  with depth ( $0.2 < R < 0.8$  at shallow depths,  $R \approx 0.0$  at the transition zone,  $R > 0.2$  at mid-crustal depths). Such changes in  $R$  may be difficult to accept if one considers that, over geologic time, some of the principal stresses should tend towards the same value because creep and slip should tend to reduce local stress deviatorics. For example,  $\sigma_3$  may remain relatively low from ongoing tectonic extension, while  $\sigma_2 \rightarrow \sigma_1$  with time. In the southern Great Basin, the reliable focal mechanisms obtained to date do not partition into depth-dependent subsets of similar type.

### Conclusions

Normal and strike-slip faulting in proximity at Black Mountain, Nevada, inferred from focal mechanisms are most easily explained by an axially symmetric stress field. Alternate explanations that also satisfy criterion II are more complicated, requiring permutations of stress directions which imply that the maximum horizontal stress increases faster with depth than the vertical stress. For the southern Great Basin region as a whole, not enough focal mechanisms have been collected

from earthquakes at mid-crustal depths (12-20 km) to constrain the stress field at those depths. At shallow depths (3-12 km), the relatively large number of predominantly strike-slip mechanisms with nearly vertical nodal planes indicate that if criterion II is satisfied and if principal stress directions are horizontal and vertical, then the maximum horizontal stress is not less than the vertical stress in magnitude.

Several limitations of this method have already been stated as assumptions: in particular that sliding is occurring on preexisting faults of favorable orientation (i.e., none of the slip data comes from newly developed fractures in intact rock). The regional southern Great Basin network has recorded few local earthquakes having  $M_L$  greater than 3.5 in the seven years of its existence; consideration of the tectonic history and mapped geology of the region strongly suggests that faults of many orientations are available for the occurrence of such low-magnitude events. For this reason, the application of the criteria and assumptions above is deemed appropriate. The presence of a variety of favorably oriented faults also should preclude the buildup of shear stresses on any planes to levels appreciably in excess of  $\mu\sigma_{eff}$ . It is this condition that sets axially symmetric stress fields apart from the others in allowing a wide variety of faulting styles to coexist. Jaeger and Cook (1969, pp 70-73) discussed a model in which  $r$  is allowed to greatly exceed  $\mu\sigma_{eff}$ , presumably because optimally oriented planes of weakness are not available, so that a range of fault-plane normal directions relative to  $\sigma_1$  is indicated, rather than the pair of directions implied by equation (3). They required  $\sigma_3 = 0.1\sigma_1$ , and  $\mu = 0.67$  to obtain the variety of fault-plane normals shown in their figure 3.8.2, for various values of  $R$ . This value of  $\mu$  is less than 50% of  $\max \frac{r}{\sigma_{eff}} = 1.42$ . In the laboratory it may be possible to generate such stress fields in rock samples, but in highly faulted *in situ* rock, large destructive earthquakes would likely occur long before  $\sigma_3 \rightarrow 0.1\sigma_1$  regionally. Also, we have already noted that shallow-depth measurements of minimum effective horizontal stress at Yucca Mountain are on the order of one-quarter the vertical stress (Stock *et al*, 1985).

Although we have not yet incorporated a joint minimization of "criterion I type-" and "criterion II type-" errors into a computer algorithm for inversion of focal mechanism data to obtain stress field parameters, we believe such a procedure is warranted. Furthermore, the application of such a program to real data samples such as are presently being collected by the southern Great Basin network should provide evidence for spatial variation in the stress field that might be ob-

scured by the less-constrained inversions presently in use. Determination of the spatial changes in the stress field is as important in the understanding of regional tectonics as is the determination of the best average stress field.

#### **Acknowledgments**

The authors wish to thank A. Michael, W. Savage and S. Sipkin for their thoughtful reviews.

The study was funded by the U. S. Department of Energy, Nevada Nuclear Waste Storage Investigations Project under Interagency Agreement DE-AI08-78ET44802.

## References Cited

- Anderson, E. M. (1951). *The Dynamics of Faulting and Dyke Formation with Applications to Britain*, 2nd ed., 206 pp., Oliver and Boyd, Edinburgh.
- Angelier, Jacques (1979). Determination of the mean principal directions of stresses for a given fault population, *Tectonophysics*, 56, T17-T26.
- Angelier, Jacques (1984). Tectonic analysis of fault slip data sets, *J. Geophys. Res.*, 89, 5835-5848.
- Ben-Menahem, A., and S. J. Singh (1981). *Seismic Waves and Sources*, 1108 pp., Springer-Verlog, New York.
- Byerlee, J. D. (1978). Friction of rocks, *Pure Appl. Geophys.*, 116, 615-626.
- Carr, W. J. (1984). Regional structural setting of Yucca Mountain, southwestern Nevada, and late Cenozoic rates of tectonic activity in part of the southwestern Great Basin, Nevada and California. USGS-OFR-84-854. 109 pp.
- Ege, J. R. (1977). *In situ* stress measured at Rainier Mesa, Nevada, and a few geologic implications. *Ph.D. Dissertation*, Colorado School of Mines, Golden, Colorado. 172 pp.
- Gephart, J. W. (1985). Principal stress directions and the ambiguity in fault plane identification from focal mechanisms, *Bul. Seism. Soc. Am.*, 75, 621-626.
- Gephart, J. W., and D. W. Forsyth (1984). An improved method for determining the regional stress tensor using earthquake focal mechanism data: application to the San Fernando earthquake sequence, *J. Geophys. Res.*, 89, 9305-9320.
- Hamilton, R. M., and J. H. Healy (1969). Aftershocks of the Benham nuclear explosion, *Bul. Seismol. Soc. Am.*, 59, 2271-2281.
- Jaeger, J. C., and N. G. W. Cook (1969). *Fundamentals of Rock Mechanics*, 515 pp. Methuen, London.
- McKenzie, D. P. (1969). The relationship between fault plane solutions for earthquakes and the directions of the principal stresses, *Bul. Seismol. Soc. Am.*, 59, 591-601.
- Michael, A. J. (1984). Determination of stress from slip data: faults and folds, *J. Geophys. Res.*, 89, 11,517-11,526.
- Morrow, C., and J. Byerlee (1984). Frictional sliding and fracture behavior of some Nevada Test Site tuffs, *Proc. U.S. Symp. Rock Mech.*, 25th, 467-474.
- Raleigh, C. B., J. H. Healy, and J. D. Bredehoeft (1972). Faulting and crustal stress at Rangely, Colorado, in *Flow and Fracture of Rocks*, AGU Monograph 16, 275-284.
- Rogers, A. M., S. C. Harmsen, W. J. Carr, and W. Spence (1983). Southern Great Basin Seismological Data Report for 1981 and Preliminary Data Analysis, USGS-OFR-83-669. 240 pp.

- Savage, W. Z., H. S. Swolfs, and P. S. Powers (1985). Gravitational stresses in long symmetric ridges and valleys, *Int. J. Rock Mech. Min. Sci. Geomech. Abstr.*, 22, 291-302.
- Sibson, R. H. (1974). Frictional constraints on thrust, wrench and normal faults, *Nature*, 249, 542-544.
- Smith, R. B. and R. L. Bruhn (1984). Intraplate extensional tectonics of the eastern basin-range: inferences on structural style from seismic reflection data, regional tectonics, and thermal-mechanical models of brittle-ductile deformation, *J. Geophys. Res.*, 89, 5733-5762.
- Stock, J. M., J. H. Healy, S. H. Hickman, and M. D. Zoback (1985). Hydraulic fracturing stress measurements at Yucca Mountain, Nevada, and relationship to the regional stress field, *J. Geophys. Res.*, 90, 8691-8706.
- Vetter, U. R., and A. R. Ryall (1983). Systematic change in focal mechanism with depth in the western Great Basin, *J. Geophys. Res.*, 88, 8237-8250.
- Zoback, M. D., and J. H. Healy (1984). Friction, faulting, and *in situ* stress, *Annales Geophysicae*, 2, 689-698.
- Zoback, M. L., and M. D. Zoback (1980a). Faulting patterns in north-central Nevada and strength of the crust, *J. Geophys. Res.*, 85, 275-284.
- Zoback, M. L., and M. D. Zoback (1980b). State of stress in the coterminous United States, *J. Geophys. Res.*, 85, 6113-6156.

U. S. Geological Survey  
Box 25046, MS 966  
Denver Federal Center  
Denver, Colorado 80225



Figure 1— Lower hemisphere focal mechanisms obtained during the years 1979 through 1983 for selected earthquakes in the southern Great Basin of Nevada and California. The mechanisms range from strike slip to normal. Near Black Mountain (BMT), the epicenters of three mechanisms, shown in the small circle, were separated by about 3 km. The estimated depths of the dip-slip earthquakes were 1 - 2 km shallower than the depths of the strike-slip earthquakes. Inverted triangles are seismograph station locations; very small circles are epicenters obtained by the seismograph network from August, 1978 through December, 1983. NTS = Nevada Test Site. The base map is from Carr (1984).

Figure 2— Pressure (P) and tension (T) axes of the 29 focal mechanisms shown in Figure 1 are plotted on a lower hemisphere equal-area projection. The pressure axes are designated as  $\sigma_3$ , and the tension axes are designated as  $\sigma_2$ .

Figure 3— (a) Geometry of a strike-slip focal mechanism and stress-field principal components plotted on a lower hemisphere equal-area projection.  $\sigma_1$ , designated as  $\bullet$ , is oriented with azimuth= $\theta^\circ$  and plunge= $0^\circ$ .  $\sigma_2$  is oriented vertically (parallel to B). The azimuth of  $\sigma_2$  is  $\theta + 90^\circ$ , and its plunge is also  $0^\circ$  ( $\circ$  symbol). Arrows indicate relative slip directions. (b) The ratio of shear stress  $\tau$  in the direction of slip ( $\tau_{xy}$  on the north-south plane,  $\tau_{yz}$  on the east-west plane) to normal stress  $\sigma$  ( $\sigma_y$  across the north-south plane,  $\sigma_z$  across the east-west plane) is computed as a function of  $\theta$ , using the directional information of Figure 3 (a) and the ratio  $\sigma_2/\sigma_1 = k$ . A fairly sharp maximum occurs for slip on the north-south plane when  $k = 0.24$  at  $\theta = 26^\circ$  (solid curve). A broader, lower maximum occurs for slip on the north-south plane when  $k = 0.316$  at  $\theta = 29^\circ$  (dashed curve).  $\tau/\sigma$  is independent of the magnitude of  $\sigma_2$  when  $\sigma_2$  is oriented in the plane of the fault, as it is here for both north-south and east-west nodal planes.

Figure 4— The stress field of figure 3 (a), where the magnitude of  $\sigma_2$  is now equal to that of  $\sigma_1$ ,  $k = 0.24$ , and  $\theta = 26^\circ$ , may be associated with all the focal mechanisms shown here, such that both criteria I and II of the text are satisfied for all of the preferred fault planes. The preferred-fault-plane strikes, dips, and rakes are listed under the corresponding mechanisms. Arrows indicate the horizontal projection of slip on the hanging wall. P and T indicate the mechanism pressure and tension directions, respectively. Only representative focal mechanisms have been shown: strike-slip,  $45^\circ$  oblique slip, and normal members. All of these kinds of deformation should be equally likely in this stress field assuming that favorably oriented planes of weakness are uniformly distributed

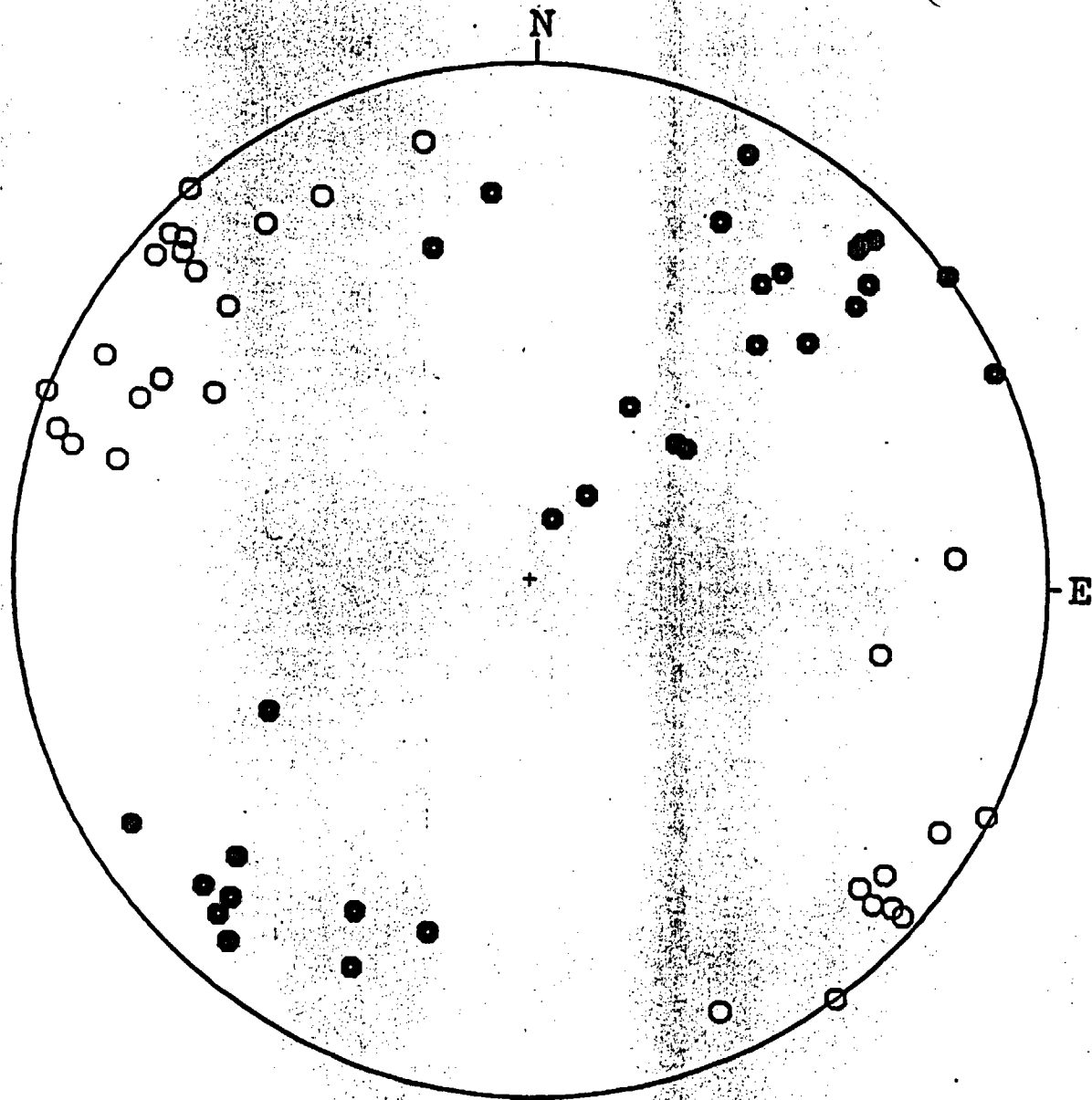
in the rock volume.

Figure 5— The stress field of figure 3 (a), where the magnitude of  $\sigma_2$  is now equal to that of  $\sigma_3$ ,  $k = 0.24$ , and  $\theta = 26^\circ$ , may be associated with these focal mechanisms, such that the slip criteria are satisfied. The preferred-fault-plane strikes, dips, and rakes are listed under the corresponding mechanisms. Arrows indicate the horizontal projection of slip on the hanging wall. P and T indicate the mechanism pressure and tension directions, respectively. Only representative focal mechanisms have been shown: strike-slip,  $45^\circ$  oblique slip, and thrust members. These kinds of deformation, sometimes observed in transitional compressional regions, are equally likely if the appropriate planes of weakness are uniformly distributed in the rock volume.

Figure 6— For the strike-slip focal mechanism of Figure 3a and the stress field in which  $\sigma_1$  is vertical;  $\sigma_2$  is horizontal, having azimuth  $N26^\circ E$ ; and  $\sigma_3$  is horizontal, having azimuth  $N64^\circ W$ ; and in which  $k = \frac{\sigma_2}{\sigma_1} = 0.24$ ,  $\frac{\tau}{\sigma}$  is plotted against  $\frac{\sigma_2}{\sigma_1}$  for the north-south slip direction (solid curve) and the east-west slip direction (dashed curve).  $\frac{\tau}{\sigma}$ , at its maximum when  $\sigma_2 = \sigma_1$ , drops rapidly to zero as  $\sigma_2 \rightarrow \sigma_3$ . On faults for which  $\mu$ , the coefficient of sliding friction, is greater than 0.6, slip on the north-south plane would be possible only when  $\sigma_2/\sigma_1 \geq 0.76$ . Slip is not indicated on the east-west plane for any  $\frac{\sigma_2}{\sigma_1}$ .



Figure 1



SGB FOCAL MECHANISMS 1979-1983

● P axis

○ T axis

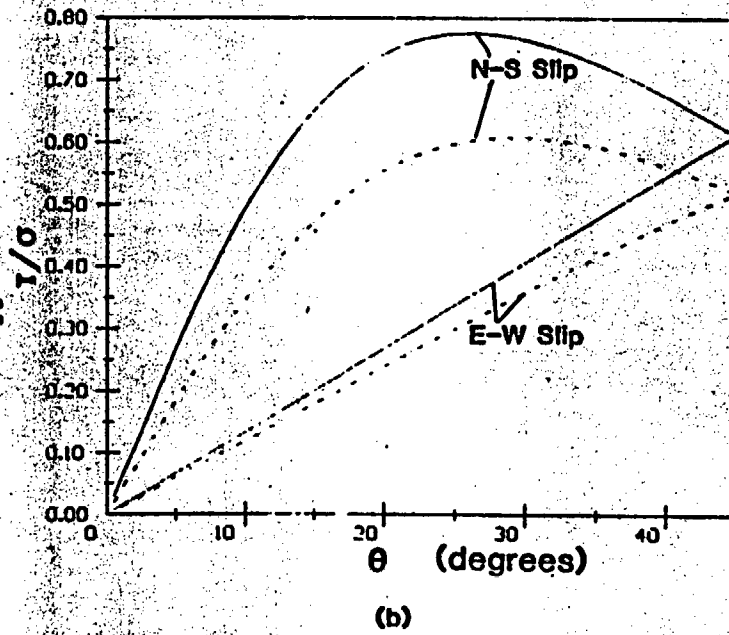
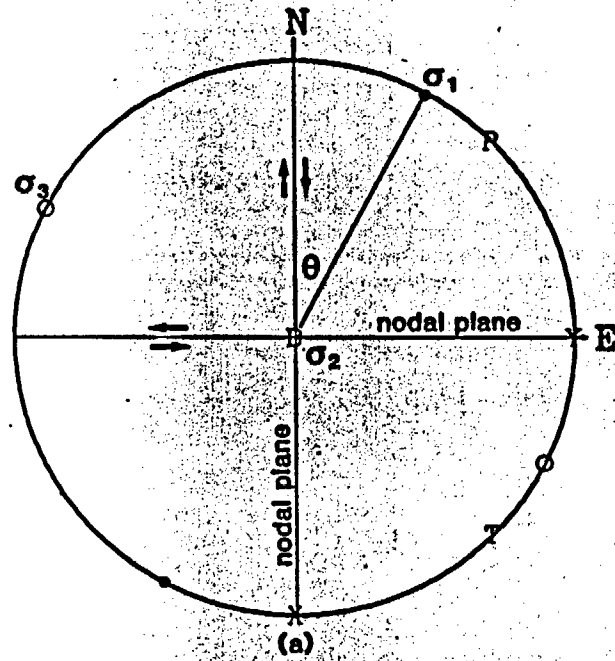
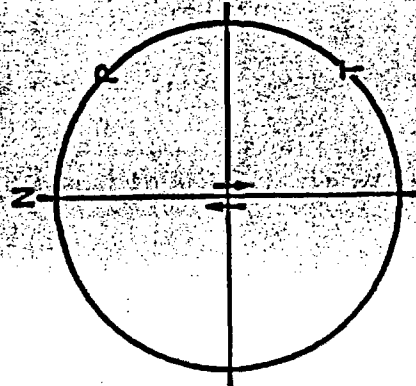
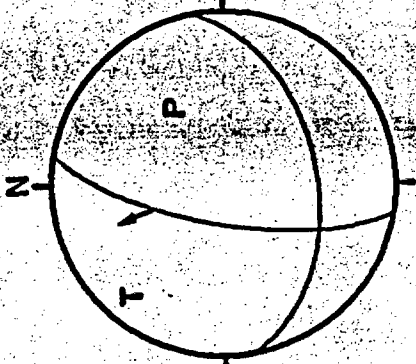


Figure 3

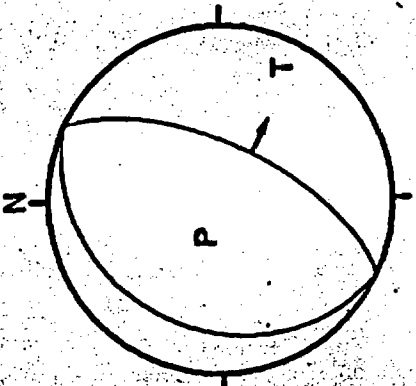
$\sigma_2 = \sigma_1$



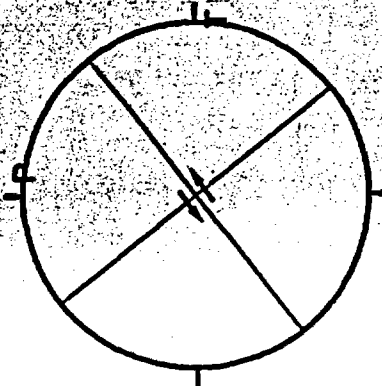
0.0°, 90.0°, 180.0°



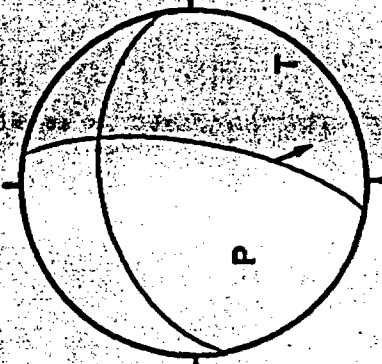
10.0°, 71.0°, 228.0°



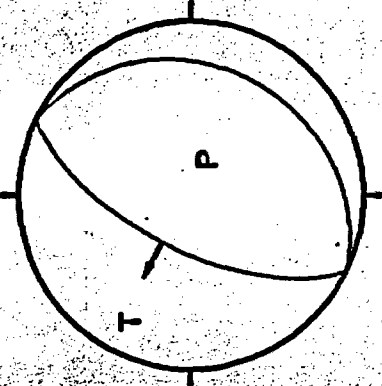
26.0°, 64.0°, -90.0°



52.0°, 90.0°, 0.0°



190.0°, 71.0°, 228.0°



206.0°, 64.0°, 90.0°

Figure 4

$$\sigma_2 = \sigma_3$$

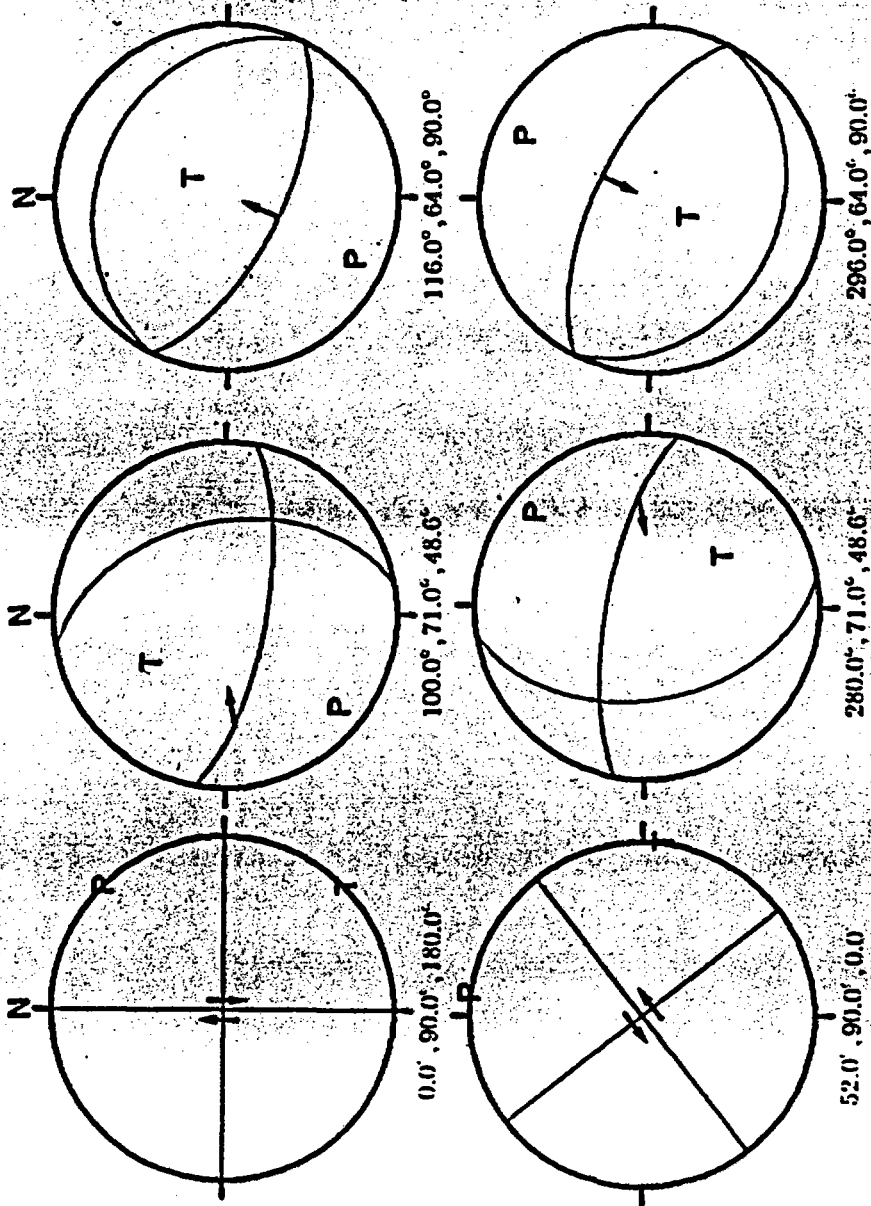


Figure 5

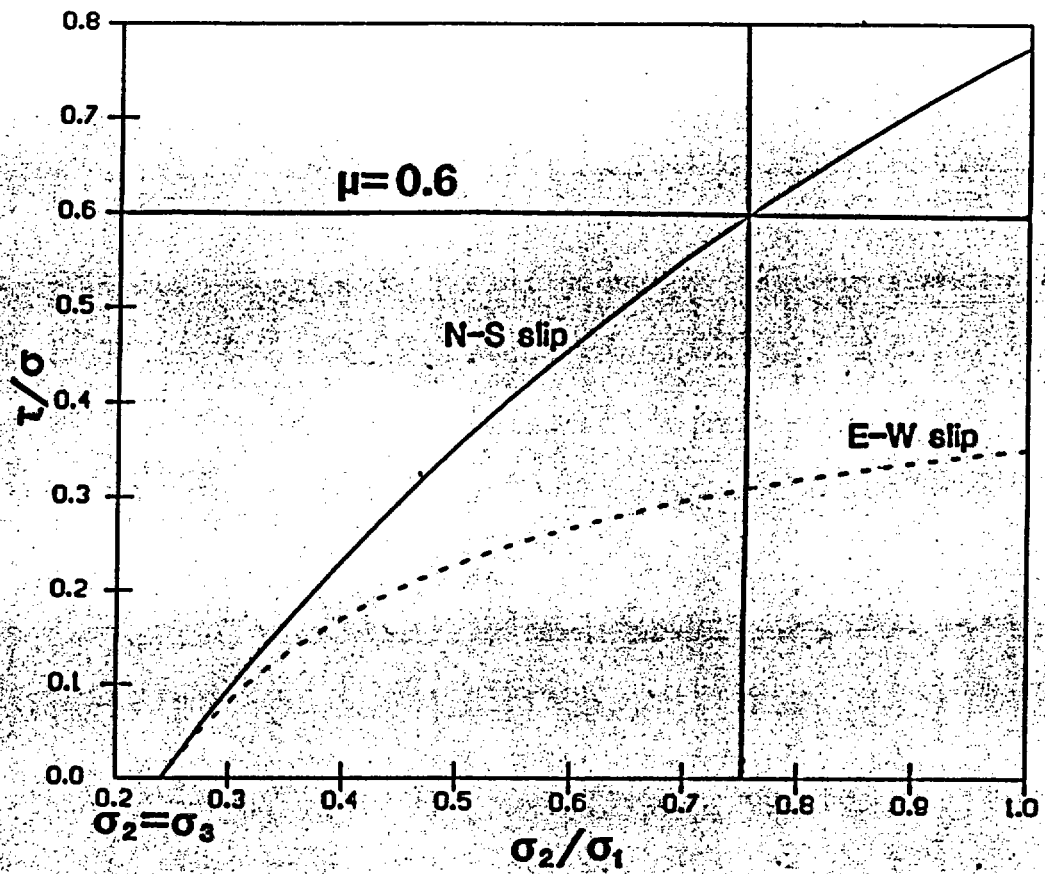


Figure 6



Persons present Tues., Aug 26, A.M.

Name	Organization	Phone
Paul Prestholt	USNRC - OR	598-6125
Charlotte Abrams	USNRC	427-4390
Keith McConnell	USNRC	427-4473
Ken Fox Jr.	USGS	236-1282
Brad Myers	USGS	(FTS) 776-1274
Terry Shideler	USGS	(FTS) 776-1418
A.K. Ibrahim	NRC	FTS 427-4211
Szymanski	DOE/NV	FTS 575-1503
BOB RAUP	USGS-GEOL DIV	FTS 776-1273
MICHAEL TEUBNER	SAIC / LV	FTS 575 1741
TERRY GRANT	SAIC / LV	FTS 575-0067
Bill Dudley	USGS	FTS 776-4920
Dore Schleicher	USGS	776-1272

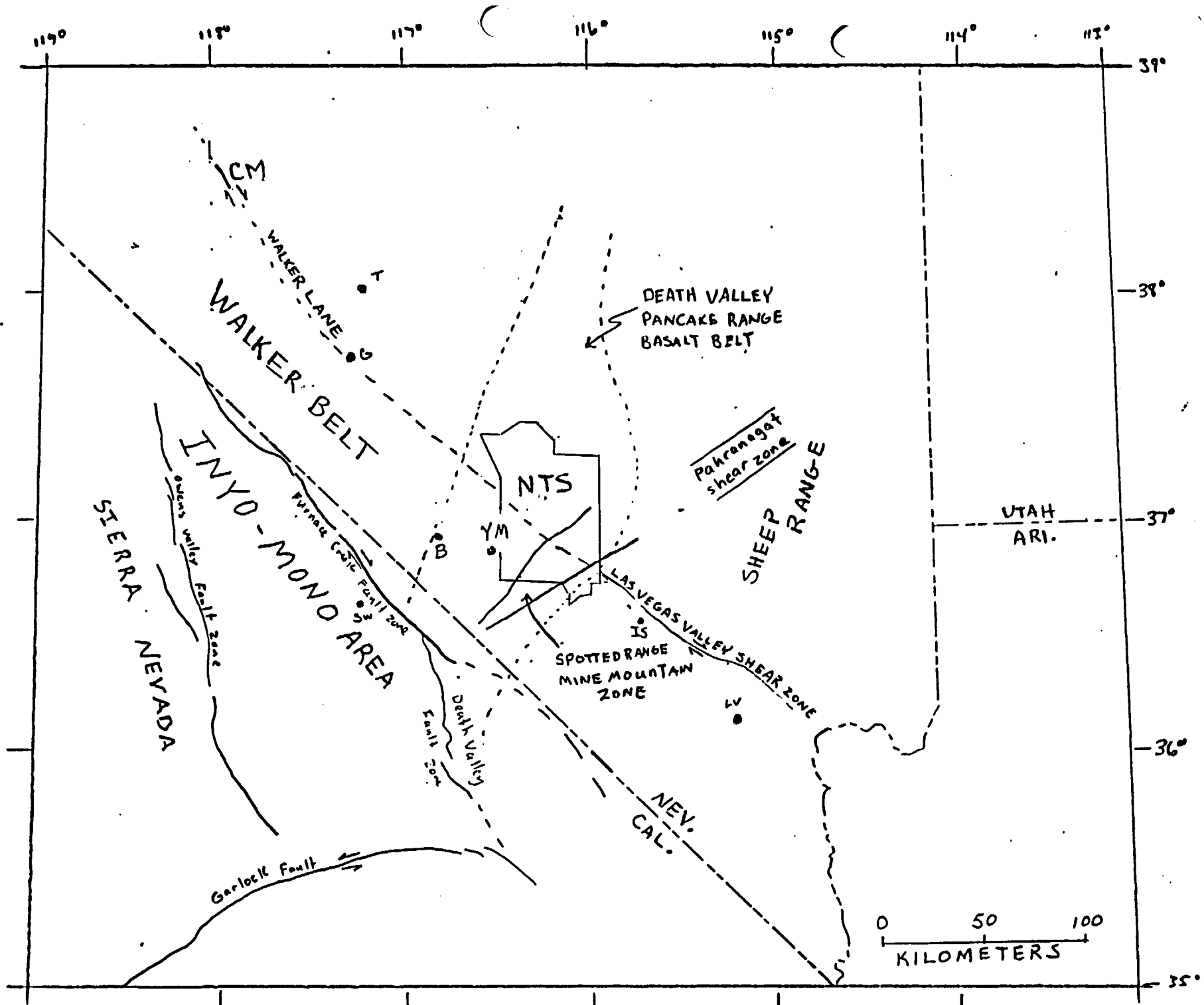


Fig. 1.20.2-3. - Regional structure map. YM, Yucca Mountain; B, Beatty; IS, Indian Springs, LV, Las Vegas; SW, Stovepipe Wells; G, Goldfield; T, Tamarack

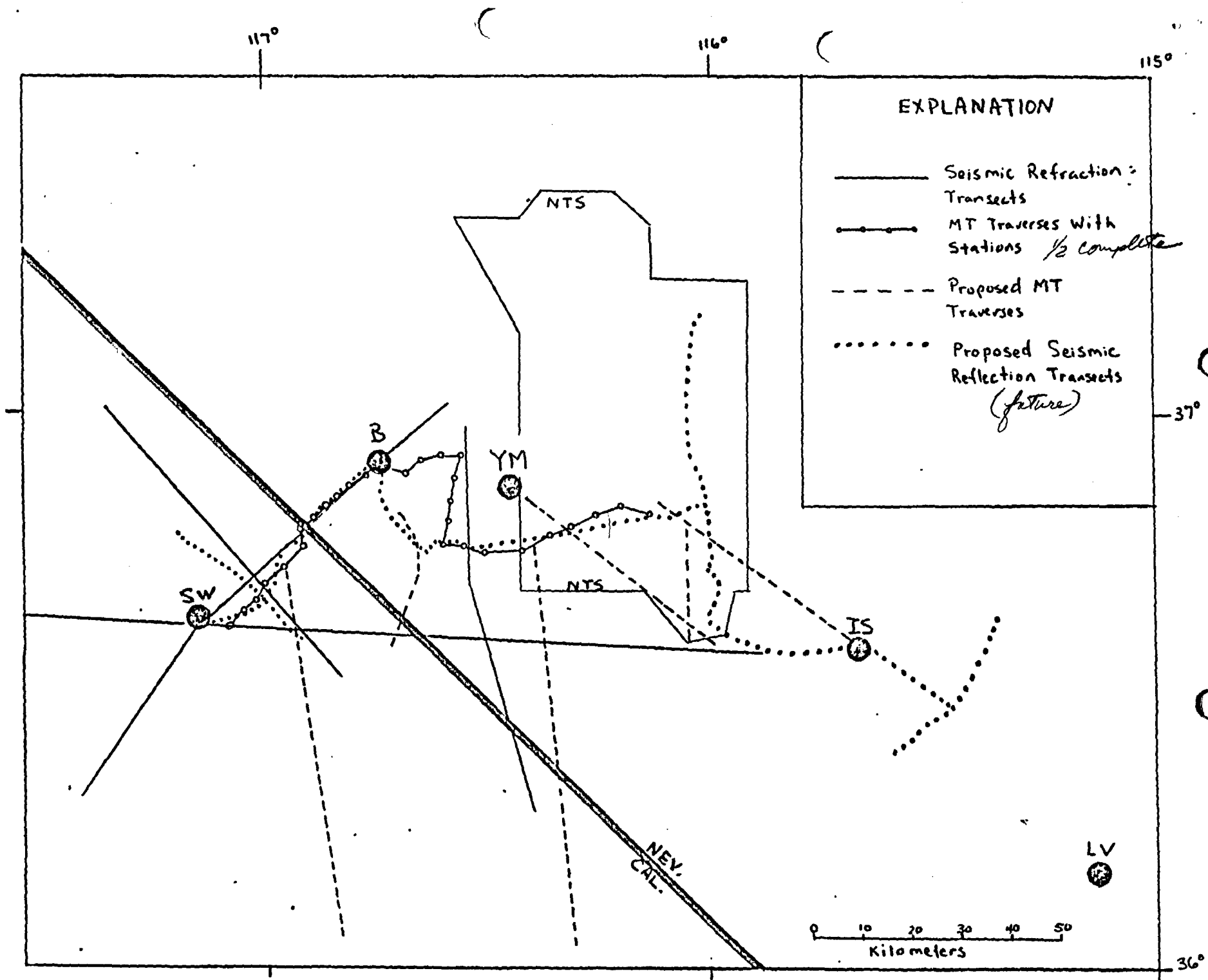


Fig. 1.20.2.-6.- Planned seismic reflection-, refraction profiles and magneto-telluric (MT) sounding traverses.

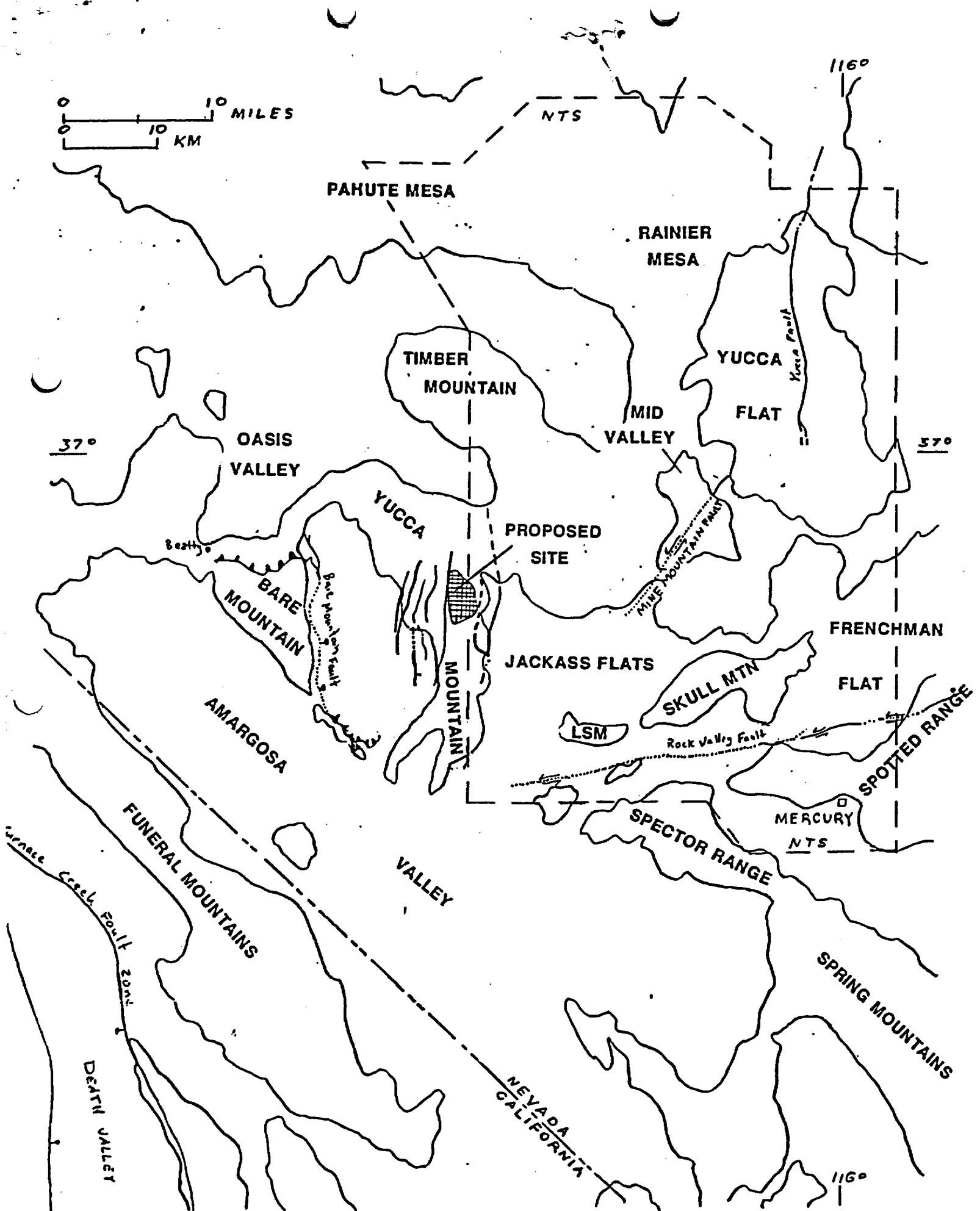


Fig. 1 20. 2-2. - Generalized Fault map of Nevada Test Site region

Quaternary

SEP 9 1986

DISTRIBUTION LIST

WM s/f  
WMGT r/f  
NMSS r/f  
REBrowning  
MJBell  
JOBunting  
PSJustus  
JStrapp  
CAbrams & r/f  
KMcConnell & r/f  
AIbrahim & r/f  
KStablein, WMRP  
JLinehan  
PPrestholt, WMRP  
RJohnson, WMRP  
PDR